Chemico-Biological Interactions 413 (2025) 111477

Contents lists available at ScienceDirect

Chemico-Biological Interactions

journal homepage: www.elsevier.com/locate/chembioint

Research paper

Potent inhibition of human monoamine oxidase A and B by phenolic compounds and polyunsaturated fatty acids in tobacco smoke

Sa Weon Hong [a,*], Ali Heydari [a], Paris R. Watson [a], Paul H. Teesdale-Spittle [b], Rachel Page [a], Peter T. Northcote [c], Robert A. Keyzers [d], Mikhail Vyssotski [e], Penelope Truman [a,f]

[a] School of Health Sciences, Massey University, Wellington, 6021, New Zealand
[b] School of Biological Sciences, Victoria University of Wellington, Wellington, 6012, New Zealand
[c] Ferrier Research Institute, Victoria University of Wellington, Wellington, 6012, New Zealand
[d] School of Chemical and Physical Sciences, Victoria University of Wellington, Wellington, 6012, New Zealand
[e] Callaghan Innovation, Gracefield Innovation Quarter, Lower Hutt, 5010, New Zealand
[f] Institute of Environmental Science and Research Ltd, Porirua, 5022, New Zealand

ARTICLE INFO

Keywords:
Monoamine oxidase inhibition
Tobacco
Catechols
Hydroquinone
PUFA
Addiction

ABSTRACT

Smoking is a main cause of premature death and preventable disease in the world. Interestingly, animal studies indicate that inhibition of monoamine oxidase (MAO), key enzymes for the degradation of neurotransmitters, increased self-administration of nicotine. The purpose of this study was to identify and characterize the potential MAO inhibitors in tobacco smoke responsible for MAO inhibition in smokers. A bioassay-guided isolation from an extract of tobacco smoke showed that catechol, 4-methylcatechol, hydroquinone, α-linolenic acid, and linoleic acid all displayed potent human MAO inhibitory activity. Additionally, the tobacco catechols 4-ethylcatechol and 4-vinylcatechol were included to test their inhibitory potencies. Catechol, 4-methylcatechol, 4-ethylcatechol, and hydroquinone are potent and irreversible MAO inhibitors. Among the phenolic compounds tested, 4-methylcatechol and 4-ethylcatechol inhibited MAO A with IC_{50} values of 10.0 and 12.6 μM, respectively, reducing to 0.27 and 0.43 μM after 1 h preincubation. In addition, α-linolenic acid and linoleic acid competitively inhibited MAO A with K_i values of 10.50 and 6.95 μM, respectively. These results suggest that MAO inhibition by phenolics and polyunsaturated fatty acids in tobacco smoke may be important contributors to the MAO inhibition experienced by smokers and to the enhancement of nicotine dependence this MAO inhibition is believed to cause.

1. Introduction

Smoking is still a major cause of premature death and is the major preventable disease in the world [1,2]. Nicotine addiction occurs when smokers become dependent on smoking for modulation of mood and arousal, relief of withdrawal symptoms, or both [3]. Like other drugs of abuse, dopamine release in the nucleus accumbens (NAc) mediates nicotine-induced pleasure and reward, which is presumed to be an important mechanism for the onset and maintenance of nicotine addiction [4]. However, animal studies suggest that nicotine has relatively weak reinforcing properties as compared to other drugs of abuse including amphetamine, cocaine or morphine [5]. It has been proposed that monoamine oxidase (MAO) inhibitors in tobacco smoke decrease the breakdown of neurotransmitters linked to the reward pathway and act synergistically with nicotine to increase the addictive effects of nicotine [6].

MAO catalyzes the degradation of a variety of monoamines, including neurotransmitters such as dopamine, serotonin, norepinephrine and epinephrine. Two isoforms, MAO A and MAO B, exist in most mammalian tissues and have different inhibitor sensitivities and substrate specificities [7]. MAO A is selectively inhibited by clorgyline and favourably oxidizes serotonin and norepinephrine, while MAO B is inhibited by selegiline (deprenyl) and oxidizes β-phenethylamine and benzylamine. Both isoforms catalyze the oxidation of dopamine, tyramine, and tryptamine [8]. However, recent studies have demonstrated that MAO A facilitates degradation of dopamine, while MAO B facilitates aberrant γ-aminobutyric acid (GABA) synthesis and hydrogen peroxide (H_2O_2) production in the pathogenesis of Parkinson's disease (PD) [9]. MAO inhibitors are currently used in medicine. Selective MAO A inhibitors are effective treatments for depression, consistent with their

* Corresponding author. School of Health Sciences, Massey University, PO Box 756, Wellington, 6140, New Zealand.
E-mail address: s.w.hong@massey.ac.nz (S.W. Hong).

https://doi.org/10.1016/j.cbi.2025.111477
Received 15 April 2024; Received in revised form 29 August 2024; Accepted 12 March 2025
Available online 13 March 2025

effectiveness in decreasing the metabolism of serotonin and norepinephrine [10], while selective MAO B inhibitors are an effective treatment for PD [11].

Surprisingly, positron emission tomography (PET) studies show that smokers have lower levels of brain MAO A (28 %; $p < 0.0003$) and MAO B (40 %; $p < 0.0002$) activity compared to non-smokers [12,13]. The mechanism of MAO inhibition in smokers is currently unknown. However, it is conceivable that several tobacco-derived substances may induce MAO inhibition in smokers, either due to additive or synergistic effects [6]. Animal studies have shown that MAO inhibition increased self-administration of nicotine [14,15], and MAO A inhibition, but not MAO B inhibition, increased self-administration of nicotine at low doses [16]. Therefore, it may be important to characterize unidentified MAO inhibitors in tobacco smoke to elucidate the mechanism of MAO inhibition and understand their contribution to the addictive effects of nicotine in humans.

Previously, a number of reversible MAO A and/or MAO B inhibitors in tobacco smoke have been studied [17–19]. The β-carboline alkaloids harman and norharman are the most well-known and potent MAO inhibitors in tobacco smoke, but these are reversible inhibitors comprise less than 10 % of the overall MAO A inhibitory activity of tobacco smoke, implying other inhibitors may contribute significantly to overall inhibitory activity [20]. On the other hand, for irreversible MAO inhibitors, Yu and Boulton [21] reported that aqueous extracts of cigarette smoke inhibited rat lung mitochondrial MAO irreversibly, suggesting that chronic use of cigarettes may act to prevent formation of neurotoxin 1-methyl-4-phenyl-1,2,3,6-tetrahydropyridine (MPTP) or MPTP-like compounds from MAO-catalyzed oxidation. Castagnoli and Murugesan [22] also found that cigarette smoke extracts reversibly and irreversibly inhibited MAO when the samples were analyzed for MAO activity after incubation for 1h. It has been suggested that identification of irreversible inhibitors from tobacco smoke is critical to fully identifying the mechanisms responsible for tobacco addiction [15].

Recently, we crossmatched an index of the chemical constituents of tobacco and tobacco smoke with existing publications of MAO inhibitory activity in search for MAO inhibitors in tobacco and tobacco smoke, and reported that 1,4-benzoquinone is the first irreversible MAO A inhibitor identified in tobacco smoke [23]. Although many studies have been conducted and have identified reversible MAO inhibitors from tobacco smoke, experimental studies on the identification of irreversible inhibitors in tobacco smoke remained unexplored until now. Since MAO inhibitors have been used clinically, identifying the responsible MAO inhibitors in tobacco smoke may be important in developing our understanding of the full psychoactive impact of tobacco smoke on smokers.

MAO inhibition in smokers may play a role in nicotine reinforcement and promote the use of tobacco products [24]. Nevertheless, it is uncertain what tobacco compounds inhibit MAO in the brain. The objective of this study was to identify and characterize the potential MAO inhibitors from tobacco smoke responsible for MAO inhibition in smokers. In this article, we report on the bioassay-guided fractionation and characterization of several MAO inhibitors (hydroquinone, catechol, 4-methylcatechol, 4-ethylcatechol, 4-vinylcatechol, α-linolenic acid and linoleic acid) identified in tobacco smoke.

2. Materials and methods

2.1. Chemicals and general procedures

All reagents were purchased from Sigma-Aldrich (St Louis, MO). The following authentic standards were obtained from Sigma-Aldrich: hydroquinone (CAS 123-31-9, order no. H3660, 99 %), catechol (CAS 120-80-9, order no. 135011, 99 %), 4-methylcatechol (CAS 452-86-8, order no. M34200, 95 %), 4-ethylcatechol (CAS 1124-39-6, order no. 683957, 95 %), α-linolenic acid (CAS 463-40-1, order no. L2376, 99 %), and linoleic acid (CAS 60-33-3, order no. L1376, 99 %). NMR spectra were acquired using a 600 MHz Varian Direct Drive spectrometer equipped with a triple-resonance HCN cryogenic probe operating at 25 K. The NMR chemical shifts (δ) were internally referenced to the residual solvent peak (δ_H 2.50, δ_C 39.53 for DMSO-d_6; δ_H 3.31 for CD_3OD; δ_H 7.26 for $CDCl_3$) [25]. Normal-phase column chromatography was achieved using silica gel and diol-functionalized silica gel (DIOL). HP20 poly (styrene-divinylbenzene) (PSDVB) chromatographic resin was used for reversed-phase column chromatography. All solvents used for liquid chromatography were of analytical or HPLC grade. Unless otherwise stated, solvent mixtures are reported as percent v/v.

2.2. HPLC-DAD-ELSD analysis

The separation and determination of relative tobacco smoke components were achieved using an Agilent Technologies 1260 Infinity HPLC coupled with a diode array detector (DAD) and an Agilent 380 evaporative light scattering detector (ELSD). A DAD was used to analyze phenolic compounds [26], while an ELSD was used to analyze compounds with no UV chromophore [27]. The separation was conducted on an Altima C18 column (250 mm × 4.6 mm, 5 μm, Alltech, USA). Mobile phases were made up of water with 0.1 % formic acid (A) and acetonitrile with 0.1 % formic acid (B). The following elution was applied: 0–25 min (linear gradient, 5–20 % B); 25–30 min (20 % B); 30–35 min (20–5 % B). The flow rate was 1 mL/min and the column temperature was 25 °C. The DAD wavelengths were set at 210, 254, and 280 nm. The ELSD parameters were as follow: evaporator temperature 40 °C; nebuliser temperature 40 °C; gas flow 1.6 L/min. The sample was filtered through a 0.45 μm syringe filter and placed into an Agilent HPLC vial. The injection volume was 10 μL.

2.3. Bioassay-guided fractionation of TPM

Bioassay-guided fractionation was conducted to identify MAO inhibitors from tobacco particulate matter (TPM). TPM was prepared using a smoking machine as previously described [28]. Briefly, tobacco (1 kg roll-your-own tobacco, "Drum" brand manufactured by Imperial Tobacco), was hand-rolled into cigarettes that each contain approximately 1 g of tobacco. Cigarettes were individually smoked, and TPM was collected onto filters using 5 cigarettes per filter. The TPM was stored on the filters at −80 °C until extraction. TPM (126.5 g) was extracted three times with MeOH (3 × 1.5 L) for 1 h. The extracts were loaded onto HP20 beads (1 L) by successive dilution with H_2O to 25 % MeOH in H_2O. The column was then eluted with 40 % MeOH/H_2O, 70 % MeOH/H_2O, 90 % MeOH/H_2O, and MeOH. For inhibition screening, each dried fraction (50 μg) was dissolved in 50 μL of EtOH, using 4 μL/100 μL reaction volume (in triplicate) to test activity. The most active fraction (MeOH fraction) was then loaded onto a DIOL column (80 mL) and eluted with increasing concentrations of CH_2Cl_2 in *n*-hexane (12.5 %–70 %), followed by CH_2Cl_2, EtOAc, and MeOH. Among them, the 70 % CH_2Cl_2/*n*-hexane and CH_2Cl_2 fractions showed the most potent MAO A inhibitory activities. These fractions were combined, loaded onto silica gel (5 mL), and eluted with 50 % CH_2Cl_2/*n*-hexane, CH_2Cl_2, and EtOAc in *n*-hexane (1 %–100 %). Finally, the two active fractions (1 % EtOAc/*n*-hexane and 10 % EtOAc/*n*-hexane) were concentrated to dryness (yield: 2.5 and 0.7 mg, respectively) for fatty acid analysis.

The 25 % MeOH/H_2O fraction, which was not retained by the column, was diluted further with water, loaded back onto fresh HP20 beads and this column was eluted with Me_2CO. The resulting fraction was concentrated to dryness (yield: 522.9 mg) and contained the highest specific MAO inhibitory activity. For these fractions, we followed the activity which increased most strongly when the fraction was pre-incubated with enzyme for 1 h. A portion (470.6 mg) of the most active fraction was then loaded onto a DIOL column (30 mL) and eluted with 50 % CH_2Cl_2/*n*-hexane, CH_2Cl_2, 10 % EtOAc/CH_2Cl_2, 25 % EtOAc/CH_2Cl_2, MeOH, and 50 % MeOH/H_2O, after which each fraction was concentrated to dryness. The 10 % EtOAc/CH_2Cl_2 fraction (27.4 mg),

providing the highest specific MAO A inhibition, was subjected to reversed-phase HPLC (see the previous Section 2.2), with a H_2O (A)/ACN (B), which afforded hydroquinone (t_R = 9.6 min, 1.1 mg), catechol (t_R = 18.2 min, 9.7 mg), and 4-methylcatechol (t_R = 29.3 min, 0.6 mg). The identities of the isolates were confirmed by spectral comparison with authentic standards.

Hydroquinone: ^{1}H NMR (CD_3OD, 600 MHz) δ 6.61 (s, 4H), 8.60 (br s, 2H, OH).

Catechol: ^{1}H NMR (CD_3OD, 600 MHz) δ 6.64–6.66 (m, 1H), 6.74–6.76 (m, 1H).

4-Methylcatechol: ^{1}H NMR (600 MHz, CD_3OD) δ 2.17 (s, 3H), 6.46 (ddq, J = 7.8, 1.8, 0.6 Hz, 1H, ArH), 6.59 (d, J = 2.0 Hz, 1H, ArH), 6.63 (d, J = 8.0 Hz, 1H, ArH), 8.59 (br s, 2H, OH).

2.4. Esterification of polyunsaturated fatty acids (PUFAs) and GC-MS analysis

To analyze PUFA composition, synthesis of fatty acid methyl esters was conducted using acid catalyzed transesterification [29] with slight modifications. The 1 % EtOAc/*n*-hexane fraction (100 μg) by silica gel chromatography was added to 1 mL of a solution of boron trifluoride (BF_3) in MeOH (14 %). This mixture was heated at 90 °C for 10 min, followed by liquid-liquid extraction with H_2O (0.5 mL) and CH_2Cl_2 (0.5 mL) three times. The combined organic phases were concentrated to dryness. EtOAc (1.5 mL) was added to the sample and analysis was conducted by GC-MS. This same procedure was repeated with the 10 % EtOAc/n-hexane fraction (100 μg).

For GC-MS analysis, a Shimadzu QP2010 Plus GCMS and AOC20i autoinjector equipped with a Restek RXI-5SilMs column (30 m length x 0.25 mm internal diameter x 0.25 μm film thickness dimensions) was used; Helium was used as the carrier gas at 1.26 mL/min constant flow (linear velocity 43.4 mL/min). Samples were injected (1 μL) into the split/splitless injector port held at 270 °C splitless mode. Upon injection, the oven was held at 150 °C for 2 min, then ramped at 4 °C/min to 300 °C and held there for 5 min, total run time 32 min. Detection was performed using an electron impact MS detector operating at 70 eV in positive ion mode. The MS transfer line was held at 305 °C, and the ion source was at 200 °C. Ions (m/z 42–600) were detected every 0.3 s, beginning at 4 min. Data were processed using Shimadzu's GCMS post-run analysis software. Compound peaks were automatically integrated using a slope of 3000 counts/min. Compounds were tentatively identified by matching to the NIST-11 and/or our in-house MS library with a minimum similarity score of 85 for annotation.

2.5. Synthesis of 4-vinylcatechol

The 4-vinylcatechol was prepared as previously described [30]. Briefly, the compound was synthesized by the decarboxylation of the starting material caffeic acid (500 mg) using sodium acetate (100 mg) as a catalyst in DMF (5 mL) at 110 °C. The reaction mixture was diluted with distilled water (50 mL) and then extracted with diethyl ether (10 mL). The organic layer was dried with anhydrous $MgSO_4$ and concentrated in vacuo. The product was purified by silica gel chromatography (3:7 EtOAc: n-hexane).

4-vinylcatechol: ^{1}H NMR (600 MHz, DMSO-d_6) δ 5.00 (dd, J = 10.9, 1.0 Hz, 1H, =CH_2), 5.49 (dd, J = 17.6, 1.1 Hz, 1H, =CH_2), 6.53 (dd, J = 12.0, 18.0 Hz, 1H, –CH =), 6.67–6.72 (m, 2H, ArH), 6.85 (d, J = 1.8 Hz, 1H, ArH), 8.95 (br s, 2H, OH); ^{13}C NMR (150 MHz, DMSO-d_6) δ 110.43, 112.88, 115.50, 118.05, 128.81, 136.76, 145.29, 145.58.

2.6. Monoamine oxidase inhibition assay

The kynuramine assay as modified from previously described methods [20,31] was used to determine MAO inhibitory activity. Human recombinant MAO A and MAO B (MAO A specific activity: 0.33 U/mg; MAO B specific activity: 0.4 U/mg; 1 U will deaminate 1 nmol of kynuramine per min at pH 7.4 at 37 °C) were purchased from Sigma Aldrich and stored at −80 °C. The reactions (final volume, 100 μL) contained phosphate buffer (50 mM, pH 7.2), kynuramine substrate (100 μM), and the test inhibitors (0.001–300 μM). The inhibitors were dissolved in EtOH (final concentration 4 % EtOH (v/v)). Controls with inhibitor and buffer only were included to remove the intrinsic fluorescence of the sample itself. Control reactions with no EtOH or inhibitor were also included. The reaction is initiated by addition of MAO (6.25 μg protein/mL) and incubated in a black microplate for 15 min (MAO A) or 30 min (MAO B) at 37 °C in an incubator. After incubation, the reaction was stopped by addition of 2.5 N NaOH (50 μL) and production of 4-hydroxyquinoline (the product of MAO-catalyzed kynuramine oxidation) monitored using a microplate reader (FLUOstar Omega, BMG Labtech) with excitation and emission at 320 and 380 nm, respectively. GraphPad Prism 8 (GraphPad Software Inc.) was used for fitting a sigmoidal dose-response curve to determine the IC_{50} values. All assays were performed in triplicate and the IC_{50} values reported as the mean ± SEM. In studies of the dependence of inhibition on incubation time, MAO A and MAO B were preincubated at 37 °C with a range of concentrations of compounds for 1h prior to kynuramine substrate addition. MAO enzyme activity was measured as described above. We used norharman, a potent inhibitor of MAO A and MAO B found in tobacco smoke, as the positive control [17].

2.7. Reversibility test and time-dependent inhibition of the phenolics

A centrifugation-ultrafiltration method was used as the primary test of reversibility [32]. First, the recombinant human MAO A enzymes (0.03 mg protein/mL) were incubated with the new inhibitors for 1h at 37 °C. Next, following an incubation, an aliquot (200 μL) was placed in an Amicon Ultra centrifugal filter (3 kDa cutoff, Millipore) and centrifuged at 16,000×g at 4 °C for 10 min, while another aliquot (200 μL) was stored in the fridge at 4 °C for the following MAO A enzyme assay. Then, the enzyme retained on the filter (3 kDa) was resuspended in phosphate buffer (50 mM, pH 7.2, 400 μL), centrifuged, and the same process repeated five times. Finally, the enzyme was resuspended in phosphate buffer (50 mM, pH 7.2, 400 μL), and then tested for MAO A activity. Control experiments were carried out to define 100 % MAO A activity. Percent (%) MAO A inhibition was calculated separately for test samples before and after washout.

To investigate the time dependence of inactivation, recombinant human MAO A enzyme (6.25 μg protein/mL) was preincubated with hydroquinone (1.0 μM), 4-methylcatechol (1.0 μM), 4-ethylcatechol (1.0 μM), catechol (1.0 μM), norharman (1.0 μM), or clorgyline (1.0 nM) for 0–3 h at 37 °C before kynuramine addition. After the preincubation time, the reaction was initiated by addition of kynuramine (100 μM) to each sample and MAO A enzyme activity was measured as described above. The inhibitors were dissolved in EtOH (final concentration 4 % EtOH (v/v)) and control with EtOH was included. Control reactions with no EtOH or inhibitor were also performed. The MAO A activity (% activity) remaining was plotted against the preincubation time to show the time dependence of MAO inactivation by the inhibitors. This analysis describes a variation of the inhibition assay described in Section 2.6. Both methods were those used during the bioassay directed purification.

2.8. ADME prediction of the phenolics

The ADME (absorption, distribution, metabolism and excretion) prediction was performed using the SwissADME (http://www.swissadme.ch) [33]. The purpose of performing ADME prediction was to assess physicochemical properties, lipophilicity, pharmacokinetics, and drug likeness of the phenolic MAO inhibitors identified from tobacco smoke. Molecular weight (MW), number of hydrogen bond acceptors (HBA) and donors (HBD), topological polar surface area (TPSA), logarithm of partial coefficient (iLogP) [34], gastrointestinal (GI)

absorption, blood-brain barrier (BBB), P-glycoprotein (Pgp) substrate, and Lipinski #violations were the parameters used in this study.

2.9. MAO enzyme kinetics of PUFAs

The purpose of performing MAO enzyme kinetics was to determine the mode of inhibition of human MAO A and MAO B by α-linolenic acid and linoleic acid. Enzyme kinetics were studied using Lineweaver-Burk and Dixon plots. MAO A (0.00625 mg protein/mL) was incubated at 37 °C for 15 min with kynuramine (20–300 μM) in the presence of α-linolenic acid (0, 10, 20, or 30 μM) or linoleic acid (0, 15, 20, or 25 μM). MAO B (0.00625 mg protein/mL or 0.0094 mg protein/mL) was also incubated at 37 °C for 30 min with kynuramine (20–300 μM) in the presence of α-linolenic acid (0, 10, or 30 μM) or linoleic acid (0, 60, 80, or 100 μM). MAO enzyme activities were measured as described for the monoamine oxidase inhibition assay. The K_i values were determined using nonlinear regression according to a competitive inhibition model. GraphPad Prism 8 was used to fit all data to the enzyme inhibition model. The K_i values are reported as the mean ± SEM (n = 3).

2.10. Molecular docking of MAO B with PUFAs

Docking simulations were conducted with Autodock Vina (v1.1.2) which is an open-source program [35,36]. To generate the protein coordinate file, the X-ray crystal structure of hMAO B in complex with safinamide (PDB ID: 2V5Z) was downloaded from the Protein Data Bank (PDB; www.rcsb.org/pdb). Water molecules, ligands and the B chain of MAO B were deleted, and polar hydrogens were added using Discovery Studio 2021 Client (https://discover.3ds.com/discovery-studio-visualizer-download). AutoDockTools (ADT) was also used for preparation of coordinate files, which included merging nonpolar hydrogens and adding Kollman charges. To prepare the ligand coordinate files, the structures of the conjugate base of α-linolenic acid (α-linolenate), the conjugate base of linoleic acid (linoleate), and the reference ligand (safinamide) were downloaded from PDB or PubChem (https://pubchem.ncbi.nlm.nih.gov). ADT computed Gasteiger charges, merged nonpolar hydrogens, and assigned atom types to each atom. A configuration file for AutoDock Vina was created, which included the receptor, ligand file name, and the docking parameters. The grid box was centered at coordinates x = 52.148, y = 156.183, and z = 28.029 for MAO B and the size of the search space was x = 26, y = 26, z = 26 with grid point spacing of 1 Å.

Molecular docking was performed to study the potential formation of the ternary MAO B–linoleate$_2$ species (EII). To generate a protein-ligand complex in PDB format, we used Cygwin (https://www.cygwin.com/), an open-source software providing useful Unix utilities to Windows environments. Docking simulations were carried out for the MAO B–linoleate complex to linoleate as described above.

2.11. Molecular dynamics simulations

In order to validate the occupancy of the PUFAs in the substrate binding site of MAO B, an extended molecular dynamics (MD) simulation was run on the docked structure of linoleic acid, using Desmond version 7.5.125 [37]. The docked structure was initially prepared using System Builder, using the SPC water model and neutralized by the addition of sodium cations. Constant pressure and temperature (NPT) molecular dynamics simulations lasting 500 ns at 300 K were run following an initial model relaxation using default settings using the OPLS4 forcefield.

2.12. Statistical analysis

Statistical analyses were conducted using GraphPad Prism software (GraphPad version 8.4.3) (GraphPad Software Inc., San Diego, CA). Data are presented as the mean ± standard error of the mean (SEM) or mean ± standard deviation (SD) for inhibition of human MAO activity analyses. Comparison between two groups was analyzed using a two-tailed Student's *t*-test. Multiple comparisons were conducted using a one-way analysis of variance (ANOVA), followed by Tukey's post-hoc test.

3. Results

3.1. Extraction and isolation

Phenols were isolated from the MeOH extract of TPM by bioassay-guided fractionation. The MeOH extracts were fractionated using reversed-phase (PSDVB, MeOH/H_2O gradient) chromatography. The 25 % MeOH/H_2O fraction was further purified using normal-phase (DIOL, EtOAc/CH_2Cl_2) chromatography. Final purification of the 10 % EtOAc/CH_2Cl_2 fraction using reversed-phase HPLC afforded the isolation of hydroquinone, catechol, and 4-methylcatechol. The structures of the compounds were identified by NMR spectroscopy such as ^{1}H NMR and ^{1}H–^{1}H correlation spectroscopy (COSY). The amounts in the final fractions were becoming too small for further fractionation, but this NMR analysis of the fractions allowed identification of major components. These were identified by spectral comparison and confirmed as the major contributors by testing of authentic standards of the identified compounds for MAO inhibitory activity. The scheme for bioassay-guided fractionation processes is shown in Fig. 1.

Further, we included 4-ethylcatechol and 4-vinylcatechol to test for their MAO inhibitory activity because they have been detected in cigarette smoke condensate [38,39] (Fig. 2) and are structurally related to catechol, although we did not isolate these compounds in our study. Four of the five compounds are commercially available. 4-Vinylcatechol was successfully synthesized from caffeic acid by thermal decarboxylation [30,40] but showed weak MAO inhibitory activity compared to other catechols. It was also expected to be unstable [41] and difficult to obtain reliable results from further research, therefore 4-vinylcatechol was not studied further.

3.2. Monoamine oxidase inhibition assay

The IC_{50} values for inhibition of human MAO A and MAO B by the four new phenolic MAO inhibitors identified in tobacco smoke are shown in Table 1. The major phenolic compounds of cigarette tar, catechol and hydroquinone, both displayed potent MAO inhibition. Tar is particulate matter from which water and nicotine have been removed [42]. Substitution with alkyl groups at the 4-position on the catechol led to improved MAO A and MAO B inhibitory activities. Inhibition of MAO A and MAO B were found to display significant time dependence. For example, the MAO A inhibition by 4-methylcatechol and 4-ethylcatechol is time-dependent, with an IC_{50} value of 10.0 and 12.6 μM, respectively, reducing to 0.27 and 0.43 μM after 1 h preincubation.

The IC_{50} values for inhibition of human MAO A and MAO B by the two new MAO inhibitors identified in tobacco smoke, which are fatty acids, are also shown in Table 1. Saturated fatty acids such as palmitic acid (C16:0) and stearic acid (C18:0) displayed no MAO A inhibition. The inhibition potencies of MAO A by *cis*-unsaturated fatty acids with two or three double bonds were more potent than that of the monounsaturated fatty acid (oleic acid) (data not shown). α-Linolenic acid and linoleic acid are both moderately potent MAO A inhibitors with IC_{50} values of 31.7 and 23.4 μM, respectively. They showed inhibitory activities against MAO B with IC_{50} values of 31.9 and 43.7 μM, respectively.

3.3. Reversibility test and time-dependent inhibition

To evaluate the reversibility of human MAO A binding by these phenolic compounds in tobacco smoke, a centrifugation-ultrafiltration method was used. We measured the MAO A inhibitory activities of

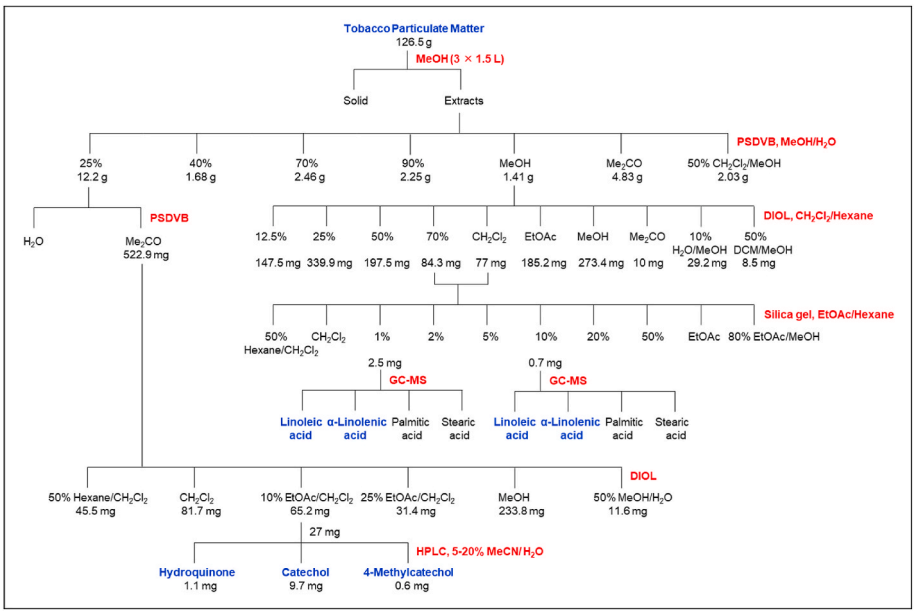

Fig. 1. Bioassay-guided isolation of phenolics and PUFAs from tobacco particulate matter.

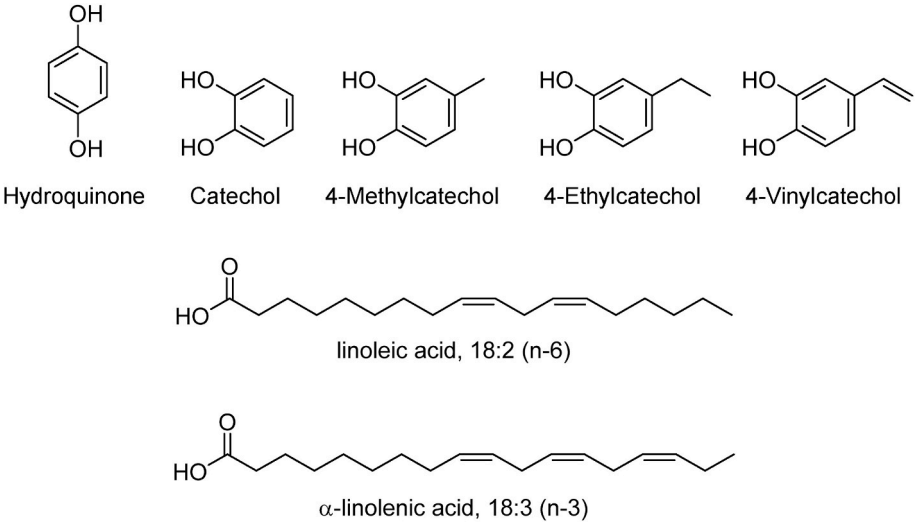

Fig. 2. Chemical structures of phenolics hydroquinone, catechol, 4-methylcatechol, 4-ethylcatechol, 4-vinylcatechol, and PUFAs α-linolenic acid and linoleic acid.

Table 1
The IC_{50} values for inhibition of human MAO A and MAO B by phenolics and PUFAs.

Compound	IC_{50} (μM), no preincubation		SI[a]	IC_{50} (μM), 1h preincubation		SI[a]
	MAO A	MAO B		MAO A	MAO B	
Hydroquinone	21.0 ± 2.36	19.7 ± 3.41	0.94	4.00 ± 0.56	3.07 ± 0.16	0.77
Catechol	34.3 ± 6.47	31.3 ± 6.13	0.91	6.69 ± 1.03	5.40 ± 2.29	0.81
4-Methylcatechol	10.0 ± 2.30	32.1 ± 5.49	3.21	0.27 ± 0.02	2.64 ± 0.19	9.78
4-Ethylcatechol	12.6 ± 3.64	27.5 ± 5.13	2.18	0.43 ± 0.03	30.7 ± 6.05	71.4
Linoleic acid	23.4 ± 2.84	43.7 ± 8.59	1.87			
α-Linolenic acid	31.7 ± 3.04	31.9 ± 5.22	1.01			
Norharman	3.55 ± 0.22	5.17 ± 0.35	1.22	3.16 ± 0.44	5.54 ± 0.32	1.75

[a] SI: selectivity index is defined as the ratio of [IC_{50} (MAO B)]/[IC_{50} (MAO A)]. The inhibition data are given as the mean ± SEM (triplicate). Control: norharman (reversible MAO inhibitor) found in tobacco smoke.

hydroquinone, 4-methylcatechol, 4-ethylcatechol, catechol, norharman, a reversible MAO inhibitor, and clorgyline, an irreversible MAO A inhibitor (Table 2). All compounds tested showed about 60–90 % inhibition of MAO A activity. After repeated washout, we found that these compounds displayed no recovery of MAO A activity, indicating that they are irreversible inhibitors of MAO A. MAO A activity was also not recovered in the assay using clorgyline as a positive control. However, norharman showed recovery of MAO A activity under identical

Table 2
Reversibility of human MAO A binding of hydroquinone and catechols.

Compound	MAO A inhibition (%)	
	before washing	after repeated washing
Hydroquinone (10 μM)	61.30 ± 0.32	63.33 ± 0.30
4-Methylcatechol (10 μM)	58.78 ± 0.63	60.94 ± 1.80
4-Ethylcatechol (20 μM)	68.83 ± 1.72	68.35 ± 0.76
Catechol (300 μM)	66.57 ± 0.66	68.92 ± 0.97
Norharman (10 μM)	87.90 ± 0.21	23.78 ± 1.73[a]
Clorgyline (5 nM)	56.06 ± 0.92	58.15 ± 0.10

The results are given as the mean ± SEM (triplicate). Controls: clorgyline (irreversible MAO A inhibitor), norharman (reversible MAO inhibitor) found in tobacco smoke. [a] Statistical significance: $P < 0.05$ compared to the corresponding % MAO A inhibition before washout of norharman, as performed by Student's *t*-test.

conditions (Table 2).

Human MAO A inhibition by hydroquinone (1.0 μM), 4-methylcatechol (1.0 μM), 4-ethylcatechol (1.0 μM), and catechol (1.0 μM) was time-dependent (Fig. 3). Among them, 4-methylcatechol showed 100 % inhibition of MAO A activity after 3 h preincubation. The results of this study suggested that these tobacco smoke components are irreversible MAO A inhibitors. MAO A inhibition with clorgyline, a positive control, was also time-dependent. In contrast, the activity of norharman, a reversible inhibitor, was not dependent on incubation time.

3.4. ADME prediction

Table 3 shows the results of *in silico* ADME prediction of the catechol and hydroquinone properties. Physicochemical descriptors such as molecular weight (MW), hydrogen bond acceptor (HBA), hydrogen bond donor (HBD), and topological polar surface area (TPSA: apparent polarity) for the phenolic irreversible MAO inhibitors are presented. For lipophilicity, the iLogP values of all compounds ranged from 0.92 to 3.43 (drug likeness criteria: between −3.93–6.46). To predict gastrointestinal absorption and brain access of the MAO inhibitors, the BOILED-Egg model from SwissADME was used (Fig. 4). Blood-brain barrier (BBB), P-glycoprotein (a drug efflux pump), TPSA, passive human gastrointestinal absorption (HIA), and WLOGP [43] are parameters used in this study. All tested compounds are predicted to show high gastrointestinal absorption (white area) (Fig. 4) and cross the blood brain barrier (yolk area) by passive penetration. In addition, all our phenolic MAO inhibitors are predicted to be non-Pgp substrates (PGP−), while harman and norharman, two known and potent MAO inhibitors from tobacco smoke, are predicted to be pumped out by Pgp (PGP+). The reference inhibitors, clorgyline and selegiline are predicted as non-substrates for Pgp (PGP−).

3.5. MAO inhibition kinetics

Lineweaver-Burk and Dixon plots were used to investigate the kinetics and mechanism of inhibition of human MAO by α-linolenic acid and linoleic acid. Lineweaver-Burk plots for the inhibition of MAO A and MAO B by α-linolenic acid were linear and intersected on the y-axis, which suggests α-linolenic acid is a competitive inhibitor of MAO A and MAO B (Fig. 5A and C). Dixon plots of the inhibition of MAO A and MAO B by α-linolenic acid were also linear (Fig. 5B and D). Lineweaver-Burk plots for the inhibition of MAO A and MAO B by linoleic acid also were linear and intersected on the y-axis, which suggests linoleic acid too is a competitive inhibitor of MAO A and MAO B (Fig. 6A and C). The Dixon plots indicated that the inhibition of MAO A and MAO B by linoleic acid was parabolic (Fig. 6B and D).

The K_i values for inhibition of human MAO A and MAO B by the two fatty acids are shown in Table 4. Kinetic analysis of inhibition by α-linolenic acid showed competitive inhibition for MAO A and MAO B, with K_i values of 10.5 μM and 16.6 μM, respectively. Linoleic acid showed parabolic competitive inhibition towards for MAO A and MAO B, with K_i values of 6.95 μM for MAO A and 40.5 μM for MAO B.

In addition, to characterize the inhibition of human MAO activity by fatty acids, GraphPad Prism 8 was used for fitting a sigmoidal dose-response curve to obtain the Hill coefficient (Hill slope). The Hill coefficient of norharman for MAO A inhibition was 0.78, whilst the Hill coefficients of α-linolenic acid and linoleic acid for MAO A inhibition were 2.22 and 2.83, respectively, suggesting positive cooperativity (Table 4).

3.6. Molecular docking

Molecular docking studies were conducted to assess the potential binding sites of α-linolenate and linoleate to hMAO B. In particular, we wished to confirm that the PUFAs could be accommodated in the substrate-binding site of MAO B, and to evaluate the potential to form a ternary complex between MAO B and two copies of linoleate, as suggested by the enzyme kinetics. Within the limitations of our proof-of-principle approach, the compounds showed the equivalent binding affinities (in the order of −8 kcal/mol) to MAO B, whereas safinamide showed a higher binding affinity (−10.3 kcal/mol).

A possible interpretation of the non-linearity of Lineweaver-Burke

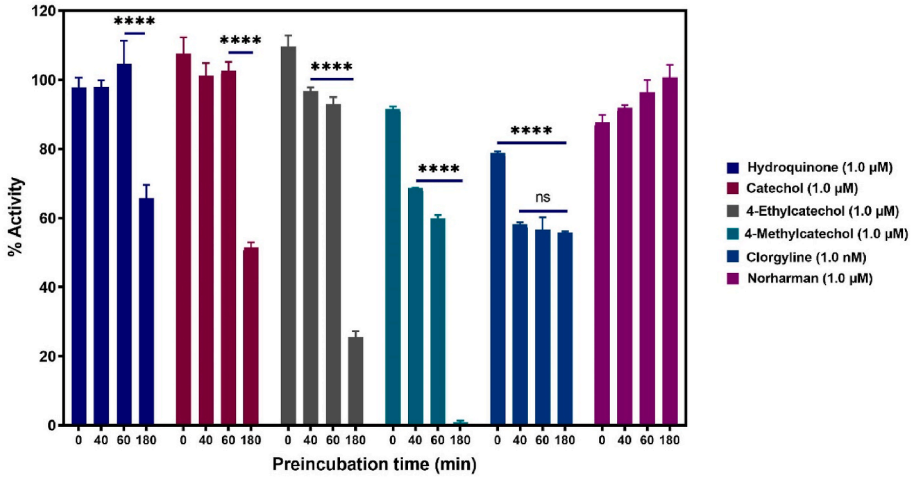

Fig. 3. Time-dependent inhibition of human MAO A by hydroquinone and catechols at concentrations well below the measured IC_{50} (see Table 1). The MAO A activity remaining is expressed as a percentage of activity in controls. The results are given as the mean ± SD (triplicate). ns, non-significant; ****$P < 0.0001$ by one-way ANOVA.

Table 3
Computed parameter values of hydroquinone and catechols in tobacco smoke.

Compound	MW	HBA	HBD	TPSA	iLogP	GI absorption	BBB	Pgp substrate	Lipinski violations
Catechol	110.11	2	2	40.46	1.13	High	Yes	No	0
4-Methylcatechol	124.14	2	2	40.46	1.39	High	Yes	No	0
4-Ethylcatechol	138.16	2	2	40.46	1.64	High	Yes	No	0
4-Vinylcatechol	136.15	2	2	40.46	1.49	High	Yes	No	0
Hydroquinone	110.11	2	2	40.46	0.92	High	Yes	No	0
Harman	182.22	1	1	28.68	1.75	High	Yes	Yes	0
Norharman	168.19	1	1	28.68	1.43	High	Yes	Yes	0
Selegiline	187.28	1	0	3.24	2.8	High	Yes	No	0
Clorgyline	272.17	2	0	12.47	3.43	High	Yes	No	0

MW: molecular weight; HBA: hydrogen bond acceptor; HBD: hydrogen bond donor; TPSA: topological polar surface area (TPSA needs to be between 20 and 130 Å^2); iLogP: for implicit log P (the logarithm of the partition coefficient between *n*-octanol and water) (iLogP should be between −3.93–6.46); GI absorption: gastrointestinal absorption; BBB: blood-brain barrier; Pgp substrate: P-glycoprotein substrate (a drug efflux pump); Lipinski: number of Lipinski's rule of five violations (drug-likeness evaluation) (maximum value: 4).

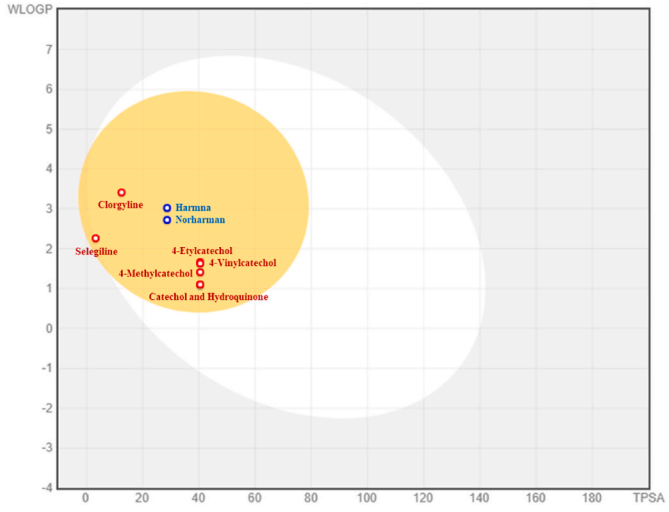

Fig. 4. Predicted BOILED-Egg representation from Swiss ADME for hydroquinone and catechols. The white area is more likely to be passively absorbed by the gastrointestinal tract, and the yellow area is more likely to penetrate the blood-brain barrier. The two areas are not mutually exclusive. The blue dot indicates P-gp substrates (PGP+) and the red dot indicates P-gp non-substrates (PGP−). WLOGP and TPSA are physicochemical descriptors for lipophilicity and apparent polarity, respectively. WLOGP is an implementation of the atomistic method from Wildman and Crippen. TPSA needs to be between 20 and 130 Å^2. Selegiline and clorgyline: irreversible MAO inhibitors. (For interpretation of the references to colour in this figure legend, the reader is referred to the Web version of this article.)

slope replots (data not shown) and Dixon plots is the formation of a ternary MAO–linoleic acid$_2$ species (EII). As enzyme kinetics indicated that linoleic acid showed competitive parabolic inhibition, Autodock Vina was used to perform the molecular docking simulation for MAO B–linoleate complex to linoleate (Fig. 8). This docking study supports the formation of the ternary MAO B–linoleate$_2$ species (EII). The binding affinity of linoleate for the MAO B–linoleate complex was calculated as −6.2 kcal/mol compared to linoleate for MAO B with a binding affinity −8.1 kcal/mol.

3.7. Molecular dynamics simulations

A 500 ns MD simulation of the docked structure of linoleate was carried out to evaluate the stability of the MAO B-associated PUFAs. Although the initial docked pose placed the carboxylate of the fatty acids proximal to the FAD coenzyme, unsurprisingly the dynamics simulation with its explicit water model reversed the orientation of the fatty acid, leaving, the hydrophobic tail of the linoleate orientated towards the FAD and the carboxylate group hydrogen bonding to bulk water and the backbone NH or side chain hydroxyl groups of the surface exposed residues Gly101, Ser 200, Thr201, and Thr202. These interactions and orientation remained stable through a further full 500 ns simulation, as represented in Fig. 7 by the 500 ns dynamics frame.

4. Discussion

In the present study, the major phenolic compounds of cigarette tar, catechol and hydroquinone, along with alkyl catechols such as 4-methylcatechol and 4-ethylcatechol displayed potent human MAO A and MAO B inhibition. Our results suggest that irreversible MAO inhibition by catechols and hydroquinone from tobacco smoke may contribute to the addictive effects of nicotine in smokers. The condensate of cigarette mainstream smoke contains significant amounts of catechol (195 μg/cigarette), hydroquinone (121.5 μg/cigarette), 4-methylcatechol (38 μg/cigarette), 4-ethylcatechol (28 μg/cigarette), and 4-vinylcatechol (84 μg/cigarette) [39] compared to norharman (2.19 μg/cigarette) and harman (0.85 μg/cigarette) [17], two previously known and potent MAO inhibitors in tobacco smoke, suggesting the phenolic compounds

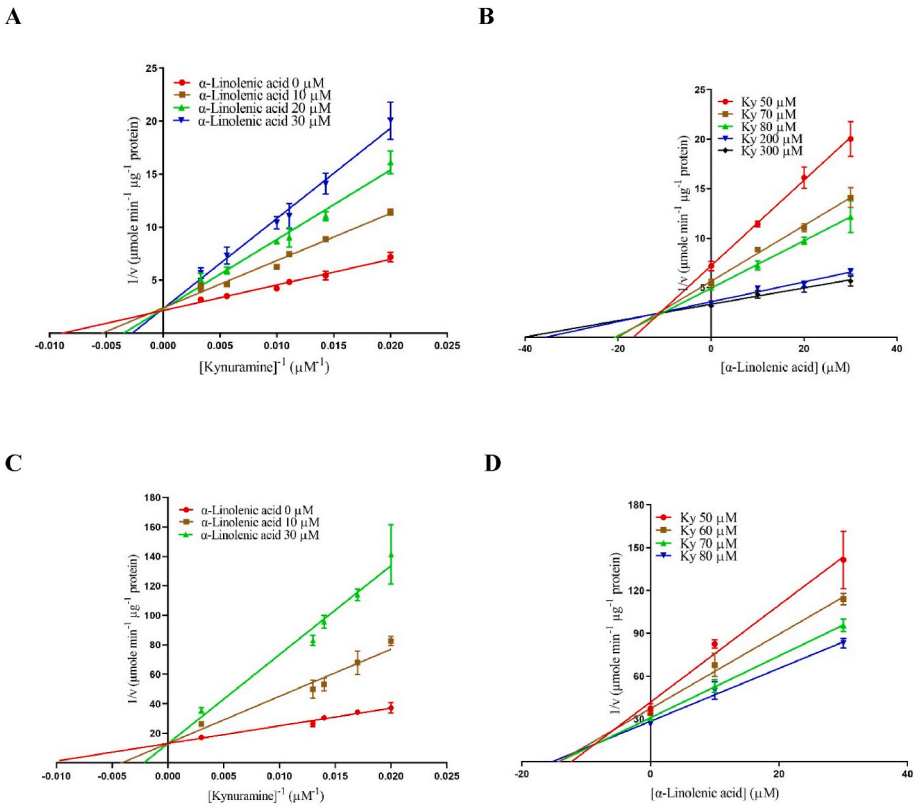

Fig. 5. Lineweaver-Burk and Dixon plots of the inhibition of MAO A and MAO B by α-linolenic acid. For MAO A, (A) and (B); and MAO B, (C) and (D). Data are given as the mean ± SD (n = 3).

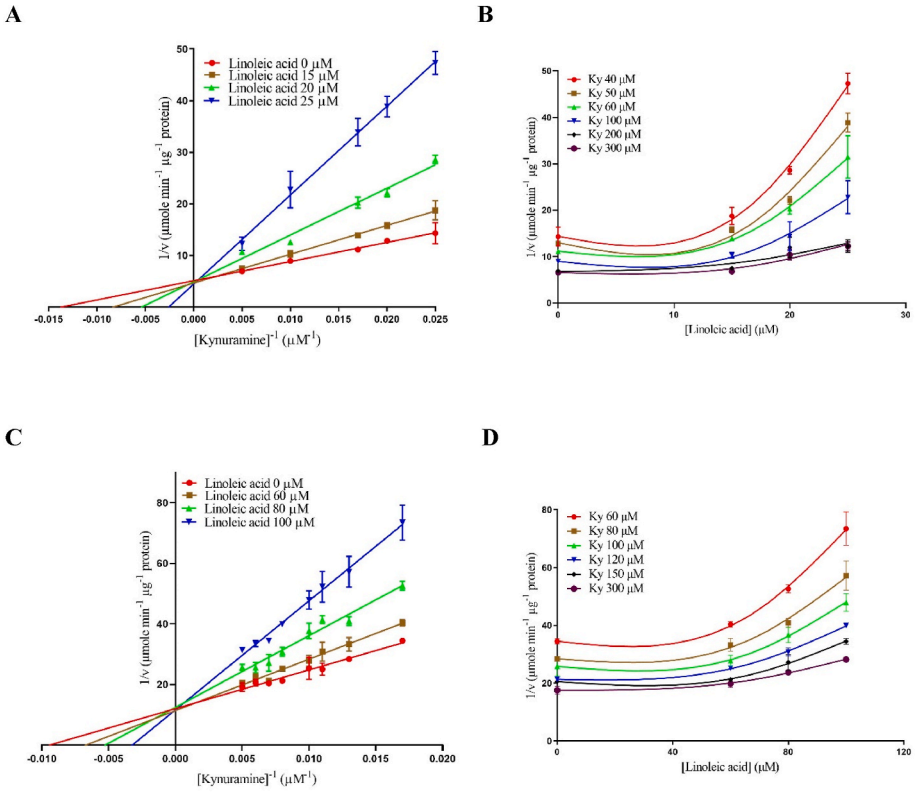

Fig. 6. Lineweaver-Burk and Dixon plots of the inhibition of MAO A and MAO B by linoleic acid. For MAO A, (A) and (B); and MAO B, (C) and (D). Data are given as the mean ± SD (triplicate).

Table 4
Inhibition of human MAO activity by α-linolenic acid and linoleic acid.

Compound	MAO A		MAO B		Mechanism of inhibition
	K_i (μM)	Hill coefficient	K_i (μM)	Hill coefficient	
Linoleic acid	6.95 ± 0.86	2.83 ± 1.13	40.5 ± 2.47	1.77 ± 0.33	Parabolic competitive
α-Linolenic acid	10.50 ± 0.99	2.22 ± 3.04	16.6 ± 1.50	1.54 ± 0.20	Competitive
Norharman	0.95 ± 0.07	0.78 ± 0.03	n.d.	1.06 ± 0.06	Competitive

The inhibition data are given as the mean ± SEM (triplicate). Hill coefficient: the cooperativity of ligand binding. Positive control; norharman: reversible MAO inhibitor found in tobacco smoke. Competitive parabolic: inhibitor (*I*) binding to a second site to form an EII complex. n.d.: not determined.

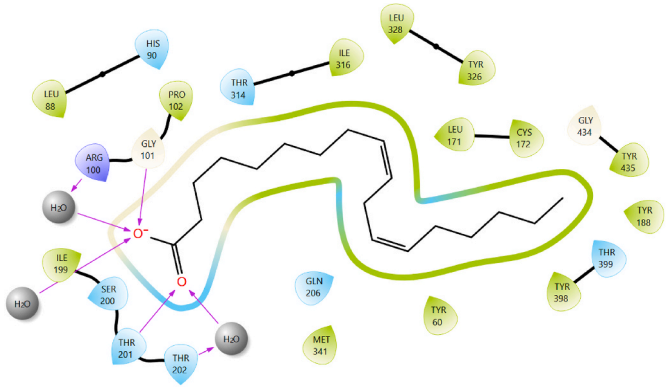

Fig. 7. Interactions of hMAO B with linoleate. The results were visualized using the Ligand Interaction Diagram routine in Maestro (Schrödinger Inc). The identity of residues in contact with the linoleate are shown. Hydrogen bonding interactions are shown as purple arrows, polar residues and surface are shown in blue shapes, and hydrophobic residues and surface are in green shapes. (For interpretation of the references to colour in this figure legend, the reader is referred to the Web version of this article.)

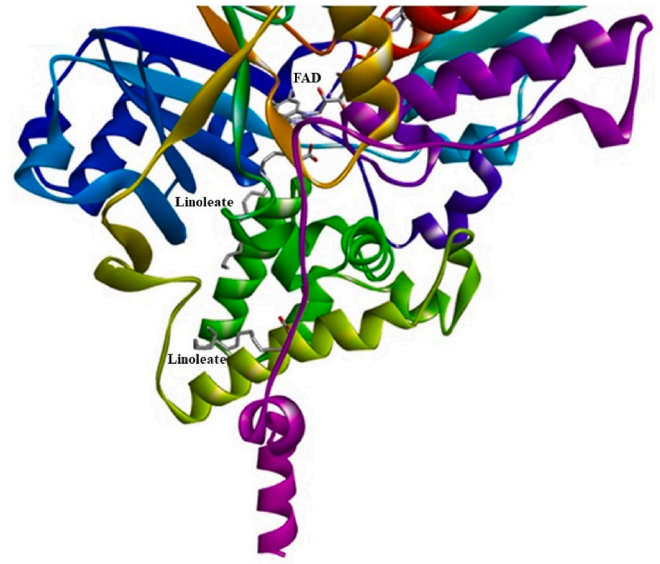

Fig. 8. Docking model of binding interaction of MAO B–linoleate$_2$ species. hMAO B is represented in ribbon form. The FAD cofactor and linoleate are represented as stick models (carbon atom in silver; oxygen atom in red). (For interpretation of the references to colour in this figure legend, the reader is referred to the Web version of this article.)

may make significant contributions to the MAO inhibitory effects of cigarette smoke because of their higher abundance in the smoke. A recent study has reported that MAO A inhibition by harman potentiates self-administration of nicotine, suggesting that harman in tobacco products contributes to addiction to smoking via MAO A inhibition [44]. However, it seems that the doses of harman in their study may have been 10-fold higher than the actual amount in tobacco smoke [45]. This result would then be congruent with that of Smith and coworkers [46] that showed that a 10-fold increase of harman's concentration could increase nicotine self-administration. Other known or unknown MAO inhibitors in tobacco smoke may play a significant role in MAO inhibition in smokers.

An earlier report stated that methylcatechol and hydroquinone from the phenolic fraction of cigarette smoke condensates displayed strong inhibitory activity on rat brain MAO B [47]. Phenolic compounds have previously been reported as reversible MAO inhibitors [48]. Phenolic compounds are known as different kinds of reversible MAO inhibitors including competitive, non-competitive, or mixed-type MAO inhibitors [49–53]. Examples of these compounds include competitive inhibitors of MAO A (flavonoids kaempferol and quercetin), MAO B (phenolic ketone paeonol), or MAO A and MAO B (phenylpropanoids eugenol and ferulic acid), non-competitive inhibitors of MAO A (paeonol), or mixed-type inhibitors of MAO B (flavonoids quercetin, quercitrin, isoquercitrin, and rutin). To our knowledge, no one has previously reported human MAO inhibition by hydroquinone, catechol, 4-methylcatechol, 4-ethylcatechol, and 4-vinylcatechol, nor shown that these compounds are irreversible inhibitors. We report for the first time that these phenolic compounds from tobacco smoke are irreversible MAO inhibitors. The findings may explain the irreversible MAO inhibitory activity of cigarette smoke [21,22].

These phenolic compounds from tobacco smoke showed irreversible MAO inhibition when analyzed using time-dependent assays for enzyme inhibition and using a centrifugation-ultrafiltration method. Irreversible MAO inhibitors are known as mechanism-based inhibitors, which have seven criteria: time dependence of inactivation, irreversibility, saturation kinetics, substrate protection, fixed stoichiometry, involvement of an enzyme-catalyzed reaction, and inactivation before release of active species [54,55]. Although these phenolic compounds meet two of these criteria, time dependence of inactivation and irreversibility, further studies are needed to confirm whether they meet the other criteria.

It is possible that catechols and hydroquinone from tobacco smoke may be converted to benzoquinones, which then form a covalent adduct with MAO enzymes. A range of catechols from natural products produce 1,2-benzoquinones (*o*-quinones) which may be responsible for the cytotoxic, genotoxic and chemopreventive effects of the catechols [56]. 1,4-Benzoquinone (*p*-quinone) is also produced via autooxidation of hydroquinone in aqueous cigarette tar extracts or via *in vivo* oxidation in living organisms [57]. Mostert et al. [58] found that human MAO A is irreversibly inactivated by 1,4-benzoquinone and other 1,4-benzoquinones, suggesting that 1,4-benzoquinones may react with the reduced FAD (flavin adenine dinucleotide) cofactor to form covalent adducts. Further structural studies are needed to describe the reactive sites of 1,4-benzoquinone in MAO A and the potential mechanism of MAO inhibition by 1,4-benzoquinone.

Our findings also suggest that catechols may play a role in the low incidence of PD in smokers. Lim et al. [47] proposed that both the suppression of MPTP-induced neurotoxicity and the low incidence of PD in smokers relative to nonsmokers could result from MAO B inhibition by cigarette smoke components. Also, catechol and its derivatives are

catechol-*O*-methyl transferase (COMT) inhibitors, and catechol was found to be both a competitive substrate of COMT and a COMT inhibitor *in vivo* [59]. Both MAO B and COMT inhibitors such as nitrocatechol derivatives are used as adjuvant drugs to levodopa (L-DOPA)-associated motor complications in PD patients [60]. As such, our findings suggest that the phenolic compounds tested in this study and other MAO B and/or COMT inhibitors (either known or unknown) in tobacco smoke may play a part in the low incidence of PD in smokers. Future studies could explore the inhibitory effects of these MAO inhibitors on cell lines such as rat pheochromocytoma (PC12) or human neuroblastoma (SH-SY5Y) cell lines, or on induced pluripotent stem cell (iPSC)-derived neural cells, which are each commonly used in Parkinson's research. Our findings suggest that further studies are necessary to test whether these MAO inhibitors are active in ameliorating PD symptoms, induced in a rodent model of PD.

In addition, we found that α-linolenic acid and linoleic acid from tobacco smoke showed potent human MAO A and MAO B inhibition. α-Linolenic acid and linoleic acid competitively inhibited MAO A with K_i values of 10.50 and 6.95 μM, respectively. The mainstream smoke of different types of cigarettes contains large amounts of α-linolenic acid (52–329 μg/g cigarette) and linoleic acid (50–146 μg/g cigarette) [61], suggesting these two PUFAs may make substantial contributions to the total MAO inhibitory activity of cigarette smoke. Even though the PUFAs we have identified in tobacco smoke are only moderately potent compared to harman/norharman, they are significant contributors because there is so much more of them than there is of harman/norharman [17]. Further research is needed to examine the contribution of the PUFAs to the total MAO inhibitory activity of cigarette smoke.

Previous studies have found significant differences in self-administration in animals when extracts of cigarette smoke were used to evaluate the reinforcing effects of non-nicotine constituents [62–64]. Levin et al. [65] suggested that the differences in the acquisition of self-administration may be attributable to lipophilic components in tobacco smoke. Further studies are required to determine whether the PUFAs affect self-administration of nicotine or cause significant MAO inhibition *in vivo*.

PUFAs are involved in the regulation of the structure and the function of neurons and non-neuronal cells such as glial and endothelial cells in the brain [66]. The PUFAs linoleic acid and α-linolenic acid, which are essential fatty acids, produce arachidonic acid (ARA), eicosapentaenoic acid (EPA), and docosahexaenoic acid (DHA), and contribute significantly to the regulation of body homeostasis of inflammation/anti-inflammation, platelet aggregation/antiaggregation, vasodilatation/vasoconstriction, and bronchoconstriction/-bronchodilation [67]. Since n–3 PUFAs, including α-linolenic acid and DHA, are able to cross the blood brain barrier via major facilitator superfamily domain-containing protein 2a (Mfsd2a) [68], α-linolenic acid from tobacco smoke may be involved in lowering MAO activity in the brains of smokers. MAO A inhibition from α-linolenic acid and linoleic acid from tobacco smoke may also lead to antidepressant action in the brains of smokers. As a consequence of selective MAO A inhibition, levels of serotonin and norepinephrine may be increased, causing clinical antidepressant action [69]. Interestingly, it has been suggested that oral n–3 PUFA intake may have a positive effect on depressive status through the potential interaction between n–3 PUFA and serotonin and dopamine neurotransmission that includes metabolism, release, absorption and receptor functions [70]. Our findings suggest that future studies should be carried out to show whether or not other n–3 PUFAs and n–6 PUFAs act as inhibitors of MAO enzymes. Of potential significance is that, during smoking, the smoke components are inhaled, rather than ingested. This allows more immediate delivery of the smoke components to the brain in higher concentrations than when the same components are ingested. However, the influence of the mode of delivery of these compounds in modulating their effects is not yet established.

Kinetic analysis revealed that linoleic acid is a competitive inhibitor of MAO A and MAO B, and the mode of MAO inhibition is parabolic competitive. Competitive parabolic inhibition is observed when inhibitor (I) binds to a second inhibition site to form an EII complex [71]. Parabolic inhibition can be parabolic competitive, parabolic uncompetitive, or parabolic noncompetitive [72]. Because linoleic acid is a competitive inhibitor of MAO and both Lineweaver-Burk slope replots and Dixon plots of linoleic acid are parabolic, these findings suggest that linoleic acid may bind to a second inhibition site to form the ternary MAO–linoleic $acid_2$ species (EII). This would help to elucidate the binding mode and inhibitory potency of linoleic acid towards MAO enzymes. The Hill coefficients of the two fatty acids for MAO inhibition were also obtained. The Hill coefficient is not only linked with the stoichiometry of enzyme–inhibitor interactions but also indicates the steepness of the dose–response relationship [73]. In the sigmoidal dose-response curve of α-linolenic acid and linoleic acid for MAO inhibition, the Hill coefficients were greater than 1. Hill coefficients greater than 1 are consistent with positive cooperativity or multiple binding sites, non-ideal inhibition behavior, or very tight-binding inhibition [73]. The high Hill coefficient of linoleic acid may arise from multiple binding sites of enzymes as enzyme kinetics indicated. Further studies are needed to describe the mechanism of MAO inhibition by α-linolenic acid and linoleic acid.

Docking simulations showed that α-linolenate and linoleate can be located at the active site of MAO B, showing the equivalent binding affinities. Although a previous docking study [74] provided comparable evidence suggesting PUFAs from fish oil inhibit MAO B and could give protection against neurological disorders, we report the stability of this interaction through extended molecular dynamics simulations. More importantly, to our knowledge, we report for the first time the biochemical investigations of α-linolenic acid and linoleic acid as MAO inhibitors.

Here, we report that phenolics and PUFAs in tobacco smoke are potent human MAO inhibitors. *In vitro* studies do not show the complexities that may be occurring *in vivo* but do provide a foundation for later studies more fully relevant to living organisms. These results show that such studies are justified and needed. The results suggest that these MAO inhibitors may play a role in reducing MAO activity in smokers. Tobacco addiction includes not only the pharmacologic effects of nicotine but also genetics, social and environmental factors [3]. In addition, research shows that tobacco smoking has been linked with MAO A inhibition in the brain of smokers [13] and that MAO A inhibition increased self-administration of nicotine at low doses in animal studies [16]. Thus, our findings suggest that MAO A inhibition by phenolics and PUFAs found in tobacco smoke may contribute to increase nicotine's primary reinforcing and reinforcement-enhancing effects in human smokers.

5. Conclusion

The aim of this study was to identify and characterize the potential MAO inhibitors in tobacco smoke that might account for the observed brain MAO inhibition in smokers. It has long been suggested that tobacco smoke results in irreversible MAO inhibition. The findings from the reversibility test, using a centrifugation-ultrafiltration method, showed that MAO A activities were not recovered by repeated washout, indicating that the phenolic compounds are irreversible inhibitors of MAO A. The results from this study show that there are irreversible MAO inhibitors present in tobacco smoke in amounts likely to be significant *in vivo*. This suggest that they may explain the irreversible MAO inhibition seen in smokers. Kinetic analysis of the MAO inhibition by the PUFA inhibitors was explored to determine the mode of inhibition. We have demonstrated that α-linolenic acid and linoleic acid are competitive inhibitors of MAO A and MAO B, and we suggest that linoleic acid may form a ternary complex, where two molecules of linoleate are associated with each molecule of the MAO enzyme. The results from this study suggest that MAO inhibition by α-linolenic acid, linoleic acid, and others

from tobacco smoke may play a role in the lower MAO activity in smokers.

Further studies will be needed to show whether these inhibitors affect tobacco dependence, in the low incidence of PD in smokers, or in the high incidence of smoking among those with a variety of mental health disorders. Overall, these findings suggest that phenolic and PUFAs inhibitors from tobacco smoke contribute significantly to the overall MAO inhibitory activity in tobacco smoke. These results provide a foundation from which to explore the effects of these inhibitors on tobacco dependence.

CRediT authorship contribution statement

Sa Weon Hong: Writing – original draft, Visualization, Validation, Methodology, Investigation, Formal analysis, Data curation, Conceptualization. **Ali Heydari:** Investigation. **Paris R. Watson:** Investigation. **Paul H. Teesdale-Spittle:** Writing – review & editing, Supervision, Investigation. **Rachel Page:** Writing – review & editing, Supervision. **Peter T. Northcote:** Supervision. **Robert A. Keyzers:** Writing – review & editing, Supervision, Investigation. **Mikhail Vyssotski:** Supervision. **Penelope Truman:** Writing – review & editing, Supervision, Resources, Project administration, Methodology, Funding acquisition, Conceptualization.

Funding

This research was funded by the University of Auckland Tobacco Control Research Tūranga, Innovation Fund, the Massey University Research Fund, the Health Research Council Explorer Fund (HRC 17/655), a Massey University PhD scholarship awarded to SW Hong, and a New Zealand Ministry of Business, Innovation and Employment Endeavour grant (MAUX1904).

Declaration of competing interest

The authors declare that they have no known competing financial interests or personal relationships that could have appeared to influence the work reported in this paper.

Data availability

Data will be made available on request.

References

[1] L.R. Gowing, R.L. Ali, S. Allsop, J. Marsden, E.E. Turf, R. West, J. Witton, Global statistics on addictive behaviours: 2014 status report, Addiction 110 (2015) 904–919, https://doi.org/10.1111/add.12899.

[2] R. West, Tobacco smoking: health impact, prevalence, correlates and interventions, Psychol. Health 32 (2017) 1018–1036, https://doi.org/10.1080/08870446.2017.1325890.

[3] N.L. Benowitz, Nicotine addiction, N. Engl. J. Med. 362 (2010) 2295–2303, https://doi.org/10.1056/NEJMra0809890.

[4] A.I. Herman, E.E. DeVito, K.P. Jensen, M. Sofuoglu, Pharmacogenetics of nicotine addiction: role of dopamine, Pharmacogenomics 15 (2014) 221–234, https://doi.org/10.2217/pgs.13.246.

[5] D.J. Balfour, The neuronal pathways mediating the behavioral and addictive properties of nicotine, in: J.E. Henningfield, E.D. London, S. Pogun (Eds.), Nicotine Psychopharmacology, Handbook of Experimental Pharmacology, Springer, Berlin, Heidelberg, 2009, pp. 209–233, https://doi.org/10.1007/978-3-540-69248-5_8.

[6] R.C. Hogg, Contribution of monoamine oxidase inhibition to tobacco dependence: a review of the evidence, Nicotine Tob. Res. 18 (2016) 509–523, https://doi.org/10.1093/ntr/ntv245.

[7] M.B. Youdim, D. Edmondson, K.F. Tipton, The therapeutic potential of monoamine oxidase inhibitors, Nat. Rev. Neurosci. 7 (2006) 295–309, https://doi.org/10.1038/nrn1883.

[8] A. Lewis, J. Miller, R. Lea, Monoamine oxidase and tobacco dependence, Neurotoxicology 28 (2007) 182–195, https://doi.org/10.1016/j.neuro.2006.05.019.

[9] M.-H. Nam, M. Sa, Y.H. Ju, M.G. Park, C.J. Lee, Revisiting the role of astrocytic MAOB in Parkinson's disease, Int. J. Mol. Sci. 23 (2022) 4453, https://doi.org/10.3390/ijms23084453.

[10] J.P. Finberg, Update on the pharmacology of selective inhibitors of MAO-A and MAO- B: focus on modulation of CNS monoamine neurotransmitter release, Pharmacol. Ther. 143 (2014) 133–152, https://doi.org/10.1016/j.pharmthera.2014.02.010.

[11] Y. Lv, Z. Zheng, R. Liu, J. Guo, C. Zhang, Y. Xie, Monoamine oxidase B inhibitors based on natural privileged scaffolds: a review of systematically structural modification, Int. J. Biol. Macromol. (2023) 126158, https://doi.org/10.1016/j.ijbiomac.2023.126158.

[12] J.S. Fowler, N.D. Volkow, G.J. Wang, N. Pappas, J. Logan, R. MacGregor, D. Alexoff, C. Shea, D. Schlyer, A.P. Wolf, D. Warner, I. Zezulkova, R. Cilento, Inhibition of monoamine oxidase B in the brains of smokers, Nature 379 (1996) 733–736, https://doi.org/10.1038/379733a0.

[13] J.S. Fowler, N.D. Volkow, G.J. Wang, N. Pappas, J. Logan, C. Shea, D. Alexoff, R. R. MacGregor, D.J. Schlyer, I. Zezulkova, A.P. Wolf, Brain monoamine oxidase A inhibition in cigarette smokers, Proc. Natl. Acad. Sci. U. S. A. 93 (1996) 14065–14069, https://doi.org/10.1073/pnas.93.24.14065.

[14] K. Guillem, C. Vouillac, M.R. Azar, L.H. Parsons, G.F. Koob, M. Cador, L. Stinus, Monoamine oxidase inhibition dramatically increases the motivation to self-administer nicotine in rats, J. Neurosci. 25 (2005) 8593–8600, https://doi.org/10.1523/JNEUROSCI.2139-05.2005.

[15] A.S. Villegier, S. Lotfipour, S.C. McQuown, J.D. Belluzzi, F.M. Leslie, Tranylcypromine enhancement of nicotine self-administration, Neuropharmacology 52 (2007) 1415–1425, https://doi.org/10.1016/j.neuropharm.2007.02.001.

[16] T.T. Smith, L.E. Rupprecht, S.N. Cwalina, M.J. Onimus, S.E. Murphy, E.C. Donny, A.F. Sved, Effects of monoamine oxidase inhibition on the reinforcing properties of low- dose nicotine, Neuropsychopharmacology 41 (2016) 2335–2343, https://doi.org/10.1038/npp.2016.36.

[17] T. Herraiz, C. Chaparro, Human monoamine oxidase is inhibited by tobacco smoke: beta- carboline alkaloids act as potent and reversible inhibitors, Biochem. Biophys. Res. Commun. 326 (2005) 378–386, https://doi.org/10.1016/j.bbrc.2004.11.033.

[18] A.A. Khalil, B. Davies, N. Castagnoli Jr., Isolation and characterization of a monoamine oxidase B selective inhibitor from tobacco smoke, Bioorg. Med. Chem. 14 (2006) 3392–3398, https://doi.org/10.1016/j.bmc.2005.12.057.

[19] A.A. Khalil, S. Steyn, N. Castagnoli Jr., Isolation and characterization of a monoamine oxidase inhibitor from tobacco leaves, Chem. Res. Toxicol. 13 (2000) 31–35, https://doi.org/10.1021/tx990146f.

[20] P. Truman, P. Grounds, K.A. Brennan, Monoamine oxidase inhibitory activity in tobacco particulate matter: are harman and norharman the only physiologically relevant inhibitors? Neurotoxicology 59 (2017) 22–26, https://doi.org/10.1016/j.neuro.2016.12.010.

[21] P.H. Yu, A.A. Boulton, Irreversible inhibition of monoamine oxidase by some components of cigarette smoke, Life Sci. 41 (1987) 675–682, https://doi.org/10.1016/0024-3205(87)90446-2.

[22] K. Castagnoli, T. Murugesan, Tobacco leaf, smoke and smoking, MAO inhibitors, Parkinson's disease and neuroprotection; are there links? Neurotoxicology 25 (2004) 279–291, https://doi.org/10.1016/S0161-813X(03)00107-4.

[23] S.W. Hong, P. Teesdale-Spittle, R. Page, P. Truman, A review of monoamine oxidase (MAO) inhibitors in tobacco or tobacco smoke, Neurotoxicology 93 (2022) 163–172.

[24] A.F. Sved, J.J. Weeks, A.A. Grace, T.T. Smith, E.C. Donny, Monoamine oxidase inhibition in cigarette smokers: from preclinical studies to tobacco product regulation, Front. Neurosci. 16 (2022) 886496, https://doi.org/10.3389/fnins.2022.886496.

[25] N.R. Babij, E.O. McCusker, G.T. Whiteker, B. Canturk, N. Choy, L.C. Creemer, C.V. D. Amicis, N.M. Hewlett, P.L. Johnson, J.A. Knobelsdorf, NMR chemical shifts of trace impurities: industrially preferred solvents used in process and green chemistry, Org. Process Res. Dev. 20 (2016) 661–667, https://doi.org/10.1021/acs.oprd.5b00417.

[26] A. Zeb, A reversed phase HPLC-DAD method for the determination of phenolic compounds in plant leaves, Anal. Methods 7 (18) (2015) 7753–7757, https://doi.org/10.1039/C5AY01402F.

[27] M. Ganzera, H. Stuppner, Evaporative light scattering detection (ELSD) for the analysis of natural products, Curr. Pharmaceut. Anal. 1 (2) (2005) 135–144, https://doi.org/10.2174/1573412054022699.

[28] T.J. Sheehan, H.J. Hamnett, R. Beasley, P.S. Fitzmaurice, Chemical and physical variations of cannabis smoke from a variety of cannabis samples in New Zealand, Forensic Sci. Res. 4 (2019) 168–178, https://doi.org/10.1080/20961790.2018.1445937.

[29] K. Eder, Gas chromatographic analysis of fatty acid methyl esters, J. Chromatogr. B Biomed. Sci. Appl. 671 (1995) 113–131, https://doi.org/10.1016/0378-4347(95)00142-6.

[30] P. Terpinc, T. Polak, N. Šegatin, A. Hanzlowsky, N.P. Ulrih, H. Abramovič, Antioxidant properties of 4-vinyl derivatives of hydroxycinnamic acids, Food Chem. 128 (2011) 62–69, https://doi.org/10.1016/j.foodchem.2011.02.077.

[31] A.J. Lewis, P. Truman, M.R. Hosking, J.H. Miller, Monoamine oxidase inhibitory activity in tobacco smoke varies with tobacco type, Tob. Control 21 (2012) 39–43, https://doi.org/10.1136/tc.2010.040287.

[32] J.H. Park, Y.H. Ju, J.W. Choi, H.J. Song, B.K. Jang, J. Woo, H. Chun, H.J. Kim, S. J. Shin, O. Yarishkin, Newly developed reversible MAO-B inhibitor circumvents the shortcomings of irreversible inhibitors in Alzheimer's disease, Sci. Adv. 5 (2019) eaav0316, https://doi.org/10.1126/sciadv.aav0316.

[33] A. Daina, O. Michielin, V. Zoete, SwissADME: a free web tool to evaluate pharmacokinetics, drug-likeness and medicinal chemistry friendliness of small molecules, Sci. Rep. 7 (2017) 42717, https://doi.org/10.1038/srep42717.

[34] A. Daina, O. Michielin, V. Zoete, iLOGP: a simple, robust, and efficient description of n- octanol/water partition coefficient for drug design using the GB/SA approach, J. Chem. Inf. Model. 54 (2014) 3284–3301, https://doi.org/10.1021/ci500467k.
[35] J. Eberhardt, D. Santos-Martins, A.F. Tillack, S. Forli, AutoDock Vina 1.2. 0: new docking methods, expanded force field, and python bindings, J. Chem. Inf. Model. 61 (2021) 3891–3898, https://doi.org/10.1021/acs.jcim.1c00203.
[36] O. Trott, A.J. Olson, AutoDock Vina: improving the speed and accuracy of docking with a new scoring function, efficient optimization, and multithreading, J. Comput. Chem. 31 (2010) 455–461, https://doi.org/10.1002/jcc.21334.
[37] K.J. Bowers, E. Chow, H. Xu, R.O. Dror, M.P. Eastwood, B.A. Gregersen, J. L. Klepeis, I. Kolossvary, M.A. Moraes, F.D. Sacerdoti, Scalable algorithms for molecular dynamics simulations on commodity clusters, in: Proceedings of the 2006 ACM/IEEE Conference on Supercomputing, 2006, pp. 84–es, https://doi.org/10.1145/1188455.1188544.
[38] J.W. Park, Analyses of phenolics in cigarette smoke by GC-MS with the multiple ion selection technique, Arch Pharm. Res. (Seoul) 5 (1982) 71–77, https://doi.org/10.1007/BF02856410.
[39] C. Smith, C. Hansch, The relative toxicity of compounds in mainstream cigarette smoke condensate, Food Chem. Toxicol. 38 (2000) 637–646, https://doi.org/10.1016/S0278-6915(00)00051-X.
[40] C.-H. Jia, J.-A. Shin, K.-T. Lee, Effects of caffeic acid phenethyl ester and 4-vinylcatechol on the stabilities of oil-in-water emulsions of stripped soybean oil, J. Agric. Food Chem. 63 (2015) 10280–10286, https://doi.org/10.1021/acs.jafc.5b02423.
[41] R. Bernini, E. Mincione, M. Barontini, G. Provenzano, L. Setti, Obtaining 4-vinylphenols by decarboxylation of natural 4-hydroxycinnamic acids under microwave irradiation, Tetrahedron 63 (2007) 9663–9667, https://doi.org/10.1016/j.tet.2007.07.035.
[42] N. Mallock, L. Böss, R. Burk, M. Danziger, T. Welsch, H. Hahn, H.L. Trieu, J. Hahn, E. Pieper, F. Henkler-Stephani, C. Hutzler, A. Luch, Levels of selected analytes in the emissions of "heat not burn" tobacco products that are relevant to assess human health risks, Arch. Toxicol. 92 (2018) 2145–2149, https://doi.org/10.1007/s00204-018-2215-y.
[43] S.A. Wildman, G.M. Crippen, Prediction of physicochemical parameters by atomic contributions, J. Chem. Inf. Comput. Sci. 39 (1999) 868–873, https://doi.org/10.1021/ci990307l.
[44] Z. Ding, X. Li, H. Chen, H. Hou, Q. Hu, Harmane potentiates nicotine reinforcement through MAO-A inhibition at the dose related to cigarette smoking, Front. Mol. Neurosci. 15 (2022) 925272, https://doi.org/10.3389/fnmol.2022.925272.
[45] P. Truman, Commentary: harmane potentiates nicotine reinforcement through MAO-A inhibition at the dose related to cigarette smoking, Front. Mol. Neurosci. 16 (2023) 1119538, https://doi.org/10.3389/fnmol.2023.1119538.
[46] T.T. Smith, M.B. Schaff, L.E. Rupprecht, R.L. Schassburger, D.M. Buffalari, S. E. Murphy, A.F. Sved, E.C. Donny, Effects of MAO inhibition and a combination of minor alkaloids, β-carbolines, and acetaldehyde on nicotine self-administration in adult male rats, Drug Alcohol Depend. 155 (2015) 243–252, https://doi.org/10.1016/j.drugalcdep.2015.07.002.
[47] H.B. Lim, H.O. Sohn, Y.G. Lee, J.Y. Moon, Y.K. Kang, Y.H. Kim, U.C. Lee, D.W. Lee, Inhibition of monoamine oxidase B by cigarette smoke constituents, J. Korean Soc. Tob. Sci. 19 (1997) 136–144.
[48] Z. Zhang, H. Hamada, P.M. Gerk, Selectivity of dietary phenolics for inhibition of human monoamine oxidases A and B, BioMed Res. Int. 2019 (2019) 8361858, https://doi.org/10.1155/2019/8361858.
[49] M.C. Gidaro, C. Astorino, A. Petzer, S. Carradori, F. Alcaro, G. Costa, A. Artese, G. Rafele, F.M. Russo, J.P. Petzer, Kaempferol as selective human MAO-A inhibitor: analytical detection in calabrian red wines, biological and molecular modeling studies, J. Agric. Food Chem. 64 (2016) 1394–1400, https://doi.org/10.1021/acs.jafc.5b06043.
[50] L. Kong, C.H. Cheng, R. Tan, Inhibition of MAO A and B by some plant-derived alkaloids, phenols and anthraquinones, J. Ethnopharmacol. 91 (2004) 351–355, https://doi.org/10.1016/j.jep.2004.01.013.
[51] M.H. Lee, R.D. Lin, L.Y. Shen, L.L. Yang, K.Y. Yen, W.C. Hou, Monoamine oxidase B and free radical scavenging activities of natural flavonoids in Melastoma candidum D. Don, J. Agric. Food Chem. 49 (2001) 5551–5555, https://doi.org/10.1021/jf010622j.
[52] V.N. Badavath, İ. Baysal, G. Uçar, S.K. Mondal, B.N. Sinha, V. Jayaprakash, Monoamine oxidase inhibitory activity of ferulic acid amides: curcumin-based design and synthesis, Arch. Pharm. 349 (2016) 9–19, https://doi.org/10.1002/ardp.201500317.
[53] G. Tao, Y. Irie, D.J. Li, W.M. Keung, Eugenol and its structural analogs inhibit monoamine oxidase A and exhibit antidepressant-like activity, Bioorg. Med. Chem. 13 (2005) 4777–4788, https://doi.org/10.1016/j.bmc.2005.04.081.
[54] R.R. Ramsay, A. Albreht, Kinetics, mechanism, and inhibition of monoamine oxidase, J. Neural Transm. 125 (2018) 1659–1683, https://doi.org/10.1007/s00702-018-1861-9.
[55] R.B. Silverman, Mechanism-based enzyme inactivators, Methods Enzymol. 249 (1995) 240–283, https://doi.org/10.1016/0076-6879(95)49038-8.
[56] J.L. Bolton, T.L. Dunlap, B.M. Dietz, Formation and biological targets of botanical o- quinones, Food Chem. Toxicol. 120 (2018) 700–707, https://doi.org/10.1016/j.fct.2018.07.050.
[57] J.B. Wooten, S. Chouchane, T.E. McGrath, Tobacco smoke constituents affecting oxidative stress, in: B.B. Halliwell, H.E. Poulsen (Eds.), Cigarette Smoke and Oxidative Stress, Springer, Berlin, Heidelberg, 2006, pp. 5–46, https://doi.org/10.1007/3-540-32232-9_2.
[58] S. Mostert, A. Petzer, J.P. Petzer, The evaluation of 1,4-benzoquinones as inhibitors of human monoamine oxidase, Eur. J. Med. Chem. 135 (2017) 196–203, https://doi.org/10.1016/j.ejmech.2017.04.055.
[59] H.C. Guldberg, C.A. Marsden, Catechol-O-methyl transferase: pharmacological aspects and physiological role, Pharmacol. Rev. 27 (1975) 135–206.
[60] J. Jankovic, M. Stacy, Medical management of levodopa-associated motor complications in patients with Parkinson's disease, CNS Drugs 21 (2007) 677–692, https://doi.org/10.2165/00023210-200721080-00005.
[61] D. Hoffmann, H. Woziwodzki, Chemical Studies on Tobacco Smoke: IV. The quantitative determination of free nonvolatile fatty acids in tobacco and tobacco smoke, Contrib. Tob. Nicotine Res. 4 (1968) 167–175, https://doi.org/10.2478/cttr-2013-0181.
[62] M.R. Costello, D.D. Reynaga, C.Y. Mojica, N.T. Zaveri, J.D. Belluzzi, F.M. Leslie, Comparison of the reinforcing properties of nicotine and cigarette smoke extract in rats, Neuropsychopharmacology 39 (2014) 1843–1851, https://doi.org/10.1038/npp.2014.31.
[63] C.A. Gellner, J.D. Belluzzi, F.M. Leslie, Self-administration of nicotine and cigarette smoke extract in adolescent and adult rats, Neuropharmacology 109 (2016) 247–253, https://doi.org/10.1016/j.neuropharm.2016.06.026.
[64] K.A. Brennan, A. Crowther, F. Putt, V. Roper, U. Waterhouse, P. Truman, Tobacco particulate matter self-administration in rats: differential effects of tobacco type, Addict. Biol. 20 (2015) 227–235, https://doi.org/10.1111/adb.12099.
[65] E.D. Levin, C. Wells, C. Pace, G. Abass, A. Hawkey, Z. Holloway, A.H. Rezvani, J. E. Rose, Self-administration by female rats of low doses of nicotine alone vs. nicotine in tobacco smoke extract, Drug Alcohol Depend. 228 (2021) 109073, https://doi.org/10.1016/j.drugalcdep.2021.109073.
[66] R.P. Bazinet, S. Layé, Polyunsaturated fatty acids and their metabolites in brain function and disease, Nat. Rev. Neurosci. 15 (2014) 771–785, https://doi.org/10.1038/nrn3820.
[67] R.K. Saini, Y.-S. Keum, Omega-3 and omega-6 polyunsaturated fatty acids: dietary sources, metabolism, and significance–A review, Life Sci. 203 (2018) 255–267, https://doi.org/10.1016/j.lfs.2018.04.049.
[68] C. Nguyen, H.-T. Lei, L.T.F. Lai, M.J. Gallenito, X. Mu, D. Matthies, T. Gonen, Lipid flipping in the omega-3 fatty-acid transporter, Nat. Commun. 14 (2023) 2571, https://doi.org/10.1038/s41467-023-37702-7.
[69] J.P. Finberg, J.M. Rabey, Inhibitors of MAO-A and MAO-B in psychiatry and neurology, Front. Pharmacol. 7 (2016) 340, https://doi.org/10.3389/fphar.2016.00340.
[70] G. Grosso, F. Galvano, S. Marventano, M. Malaguarnera, C. Bucolo, F. Drago, F. Caraci, Omega-3 fatty acids and depression: scientific evidence and biological mechanisms, Oxid. Med. Cell. Longev. 2014 (2014), https://doi.org/10.1155/2014/313570.
[71] F. Antunes, H.S. Marinho, M.C. Barreto, M.L. Pavao, R.E. Pinto, Diagnosis of enzyme inhibition based on the degree of inhibition, Biochim. Biophys. Acta Gen. Subj. 1624 (2003) 11–20, https://doi.org/10.1016/j.bbagen.2003.08.007.
[72] W. Cleland, The kinetics of enzyme-catalyzed reactions with two or more substrates or products: II. Inhibition: nomenclature and theory, Biochim. Biophys. Acta (BBA) - Spec. Sect. Enzymol. Subj. 67 (1963) 173–187, https://doi.org/10.1016/0926-6569(63)90226-8.
[73] R.A. Copeland, Evaluation of Enzyme Inhibitors in Drug Discovery: a Guide for Medicinal Chemists and Pharmacologists, John Wiley & Sons, Inc., New Jersey, 2013, https://doi.org/10.1002/9781118540398.
[74] M. Maria, S. Erum, N. Sadaf, Evaluation of inhibitory potential of PUFAs from fish oil against monoamine oxidase-B: a molecular docking study, Int. J. Biol. Biotech. 16 (2019) 901–909. https://www.cabdirect.org/globalhealth/abstract/20203230297.